Available online at www.sciencedirect.com
SCIENCE DIRECT
Journal of Pharmaceutical and Biomedical Analysis 40 (2006) 1097–1104
JOURNAL OF PHARMACEUTICAL AND BIOMEDICAL ANALYSIS
www.elsevier.com/locate/jpba

# Structure elucidation and conformational study of V8 A novel synthetic non peptide $AT_1$ antagonist

Panagiotis Zoumpoulakis [a], Aggeliki Politi [a], Simona Golic Grdadolnik [c], John Matsoukas [b], Thomas Mavromoustakos [a,*]

[a] *National Hellenic Research Foundation, 48 Vas. Constantinou Ave. 11635, Athens, Greece*
[b] *Department of Chemistry, University of Patras, Rio, Greece*
[c] *National Institute of Chemistry, Hajdrihova 19 P.O. Box 30 SI-1115, Ljubljana, Slovenia*

Received 14 July 2005; received in revised form 1 September 2005; accepted 5 September 2005
Available online 2 November 2005

**Abstract**

$AT_1$ antagonists constitute the most recent class of antihypertensive drugs which act through the Renin Angiotensin System (RAS). In an effort to comprehend their stereoelectronic features, a study was initiated to compare the conformational properties of drugs already marketed for the treatment of hypertension with synthetic ones, possessing common structural characteristics. In this study, the synthetic $AT_1$ antagonist V8 is structurally elucidated and its conformational properties are studied through a combination of NMR spectroscopy and computational analysis. Its conformational properties are compared with those of the structurally similar prototype $AT_1$ antagonist losartan.


*Keywords:* Synthetic angiotensin II antagonists; Conformational properties; Molecular modeling; NMR; Losartan

## 1. Introduction

The Renin Angiotensin System (RAS) plays a determinant role in the regulation of blood pressure. The octapeptide hormone angiotensin II is the active product of RAS which causes vasoconstriction when binds to $AT_1$ receptor. Angiotensin Converting Enzyme (ACE) and Renin inhibitors were first designed to block the formation of angiotensin II and angiotensin I, correspondingly. $AT_1$ antagonists constitute the most recent class of them. They block the receptor in a competitive or insurmountable way so that angiotensin II cannot bind at the active site.

Potent $AT_1$ antagonists are designed to mimic the C-terminal segment of angiotensin II [1–6]. The first non peptide $AT_1$ receptor antagonist successfully entered the market was losartan (COZAAR), developed in 1995 by Dupont Merck Pharm. Up to now, all $AT_1$ antagonists (SARTANS) which are pharmaceutical products, are derivatives of losartan.

Our previous work was concentrated to study the relationship between conformation and bioactivity in $AT_1$ antagonists. To achieve this aim, the conformational analysis of peptides and peptidomimetic both commercial and synthetic analogs have been studied [7–10]. In addition, a two-step model was proposed for the action of $AT_1$ antagonists involving first their incorporation into membrane bilayers and then lateral diffusion into the active site [11]. The conformational analysis of $AT_1$ antagonists in various solvents of polar, amphipathic and hydrophobic nature showed that the environment did not differentiate significantly their preferred low energy conformation [12,13]. Biophysical studies in micelles or liposomes aimed to detect their topography and conformation in a membrane simulating environment as well as preliminary computational analysis results on these environments point out that the preferred conformations of $AT_1$ antagonists are almost indistinguishable with that observed in solvent environments. Theoretical docking calculations showed that $AT_1$ antagonists preserve their conformation when interact with $AT_1$ receptor. These results justify that solvent, membrane or receptor simulating environments are not critical for drug conformation and therefore one can justify a discussion which relates their conformation with bioactivity [14,15]. However, it does not escape our attention that a differentiation of conformation may occur in the biological environment when they are bound to the receptor (bound-state). This issue will be addressed

* Corresponding author. Fax: +30 10 7273831.
*E-mail address:* tmavro@eie.gr (T. Mavromoustakos).

0731-7085/$ – see front matter © 2005 Elsevier B.V. All rights reserved.
doi:10.1016/j.jpba.2005.09.016

when 3D QSAR studies will be applied after the synthesis of a sufficient amount of this class of synthetic molecules. If a proper relationship between conformation and bioactivity is observed it will justify the above findings. Otherwise, it will show the dynamic effect of the receptor which causes conformational changes to the drug during the binding.

The structural features which determine the pharmacophoric segments of losartan have been examined in a previous study [10]. These are: (a) conformation of the biphenyl tetrazole moiety; (b) orientation of the hydroxymethylimidazole relative to the biphenyl template; (c) the conformation of the butyl chain and its orentation toward the biphenyl group. Superimposition of losartan with the C-terminal region of the peptide $AT_1$ antagonist sarmesin, showed that: (i) losartan's hydroxymethylimidazole matched with sarmesin's imidazole of $His^6$; (ii) losartans's *n*-butyl chain was in spatial proximity with *n*-butyl chain of sarmesin's $Ile^5$ carbon chain; (iii) losartan's spacer phenyl ring matched with sarmesin's pyrrolidine group of $Pro^7$. Interestingly, losartan mimics the γ-turn formed around $Pro^7$ in sarmesin.

In the present study, an angiotensin II $AT_1$ antagonist (V8) is structurally elucidated and its conformational properties are compared to those of losartan (Fig. 1). The antihypertensive effect and the degree of potency of V8 were tested in vivo in a preparation of anesthetized rabbits made hypertensive by AII infusion. V8 possessed a dose-dependent AII antagonistic effect at the doses of 2 and 3.5 μmol comparable to those of losartan. In vitro binding studies showed that V8 had high affinity for the $AT_1$ receptor and more specifically in the range of nanomolar as losartan ($IC_{50}$ of V8 $53.8 \pm 6.4$ nM and $IC_{50}$ of losartan $16.4 \pm 1.6$ nM) [16]. V8 like losartan did not show binding to $AT_2$ receptor indicating that it is a selective $AT_1$ antagonist.

Comparing the structures of V8 with losartan, the positions of butyl alkyl chain and hydroxymethyl substituents in the imidazole ring of V8 are reversed. The imidazole ring of V8 devoids the chlorine atom.

## 2. Materials and methods

### 2.1. Materials

DMSO-$d_6$ and ultra precision NMR tubes Wilmad 535-5 mm (SPINTEC ROTOTEC) were used for the NMR experiments.

### 2.2. Nuclear magnetic resonance spectroscopy

V8 was dissolved in DMSO-$d_6$ and a series of experiments were performed using Varian INOVA 600 MHz and Bruker AC 300 instruments at 300 K. All data are collected using pulse sequences and phase-cycling routines provided in the Bruker and Varian libraries of pulse programs. Data processing including sinebell apodization, Fourier transformation and phasing, were performed using Varian and Bruker software packages. The DQF-COSY, $^1H$–$^{13}C$ HSQC and $^1H$–$^{13}C$ HMBC experiments were performed with gradients [17–19]. The ROESY experiment was recorded using standard pulse sequence in the phase-sensitive mode and was measured at 150 ms mixing time. The $^1H$ sweep width was 9820 at 600 MHz [20]. Typically the homonuclear proton spectra were acquired with 4096 data points in $t_2$, 16–64 scans, 256–512 complex points in $t_1$ and a relaxation

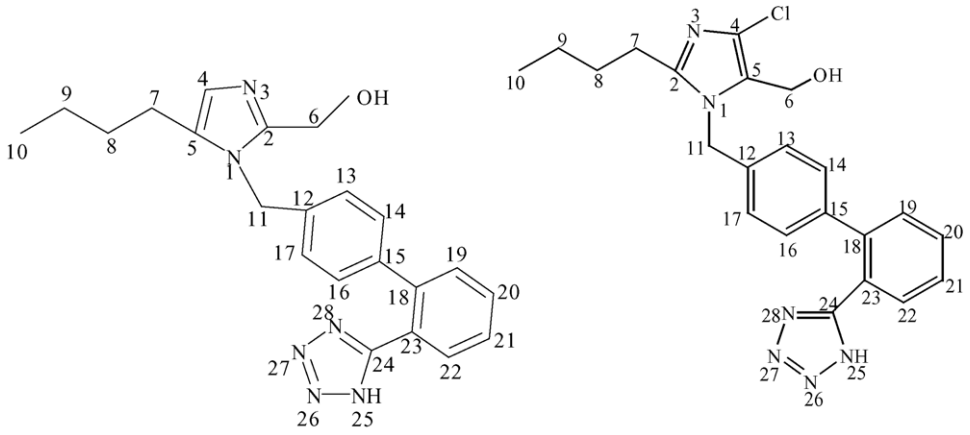

V8 Losartan

**Dihedral angles of V8**

$\tau_1$= C18-C23-C24-N25
$\tau_2$= C19-C18-C15-C14
$\tau_3$= C17-C12-C11-N1
$\tau_4$=C12-C11-N1-C2
$\tau_5$=N1-C2-C6-O
$\tau_6$=C2-C6-O-H
$\tau_7$=C8-C7-C5-N1
$\tau_8$=C9-C8-C7-C5
$\tau_9$=C10-C9-C8-C7

Fig. 1. Chemical structures of the $AT_1$ antagonists V8 and losartan. Underneath are displayed the dihedral angles for the V8 antagonist.

delay of 1–1.5 s. The $^{1}H$–$^{13}C$ HSQC spectrum was recorded with 1024 data points in $t_2$, 16 scans per increment, 128 complex pints in $t_1$ and a relaxation delay of 1 s. The $^{1}H$–$^{13}C$ HMBC spectrum was recorded with 4096 data points in $t_2$, 64 scans per increment, 512 points in $t_1$ and a relaxation delay of 1 s [21,22]. The $^{13}C$ spectral width was 20,000 and 30,000 Hz for the HSQC and HMBC experiments, respectively. Distances were calculated from cross-peak volumes in ROESY spectra using the VNMR program and a ±10% was applied to produce the upper and the lower limit constraints.

### 2.3. Molecular modeling

Computer calculations were performed using Quanta software of Molecular Simulations on a Silicon Graphics $O^2$. Molecular Mechanics calculations were carried out using the CHARMm force field. V8 was first minimized with steepest descents and then with Newton–Raphson algorithms using an energy tolerance of 0.01 kcal $mol^{-1}$ $A^{-1}$, to reach a local minimum. The dielectric constant ($e$) was set to 45 during minimization simulating the DMSO environment. To generate random conformers, a systematic search procedure (random sampling) was applied. This method randomly changes all defined torsion angles within a predefined angular window. The range of the torsion angle varies during the search procedure and generates new conformations. CHARMm energy minimization is performed for each randomly altered conformation. In order to explore the preferred torsion angles that correspond to the lowest energy conformers and energy barriers of V8, stochastic search procedures (systematic grid scan) were used. This method initiates a grid scan search that generates conformations by varying specified torsion angles over a grid of equally spaced values. Intervals of 5° were applied for single bond rotation and 10° of two bond rotation. During these searches, the predetermined torsion angle remained constant while minimization using 1000 steps of conjugate gradient algorithm was applied to "relax" the whole molecule.

Molecular Dynamics simulations on V8 were carried out at 1000.0 K using CHARMm force field. A time step of 1 fs for 300 ps using an output frequency of 1 ps to sample 300 frames of conformers was employed for the MD simulation. The simulation protocol consisted of two minimization cycles (steepest descent and conjugate gradient) first with the solute fixed and then with all the atoms allowed to move free. The NMR distance constrains were applied during the complete simulation with a force constant of 10 kcal $mol^{-1}$ $Å^{-1}$.

## 3. Results and discussion

### 3.1. Structure elucidation of V8

Fig. 2 depicts the $^{1}H$ NMR spectrum of V8 in DMSO-d6. This solvent was found to be appropriate for the simulation of the amphiphilic environment of the $AT_1$ receptor in the membranes [5]. Observed peaks are referenced to TMS. The assignment of the peaks is shown on the top of them. The proton chemical shifts are assigned following standard procedures using homonuclear DQF-COSY and ROESY spectra (Fig. 3; Table 1).

Interesting to note is the main peak at 7.116 ppm accompanied by two small side peaks which is attributed to four protons of the phenyl ring attached to the imidazole. The spin system

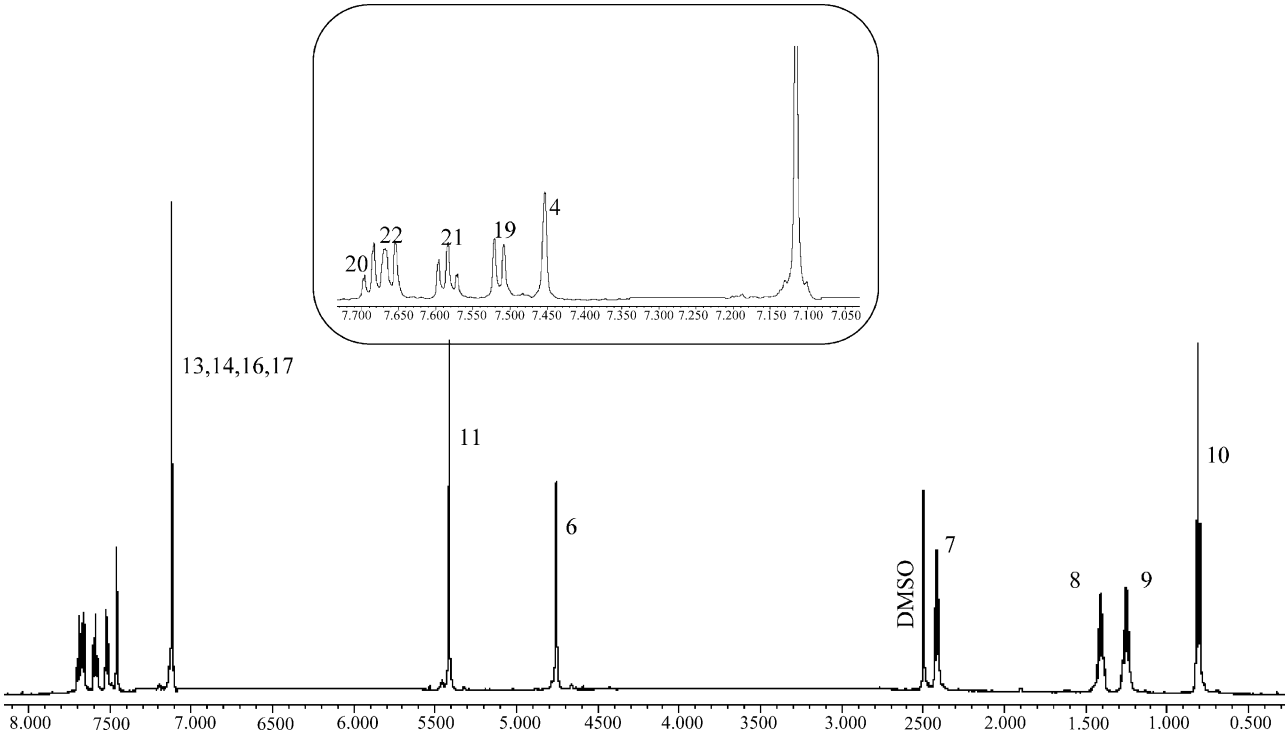


Fig. 2. $^{1}H$ NMR spectra of V8 in DMSO solvent, recorded on a Varian INOVA 600 MHz spectrometer at a temperature of 25 °C. Inset shows an expansion of the aromatic region.

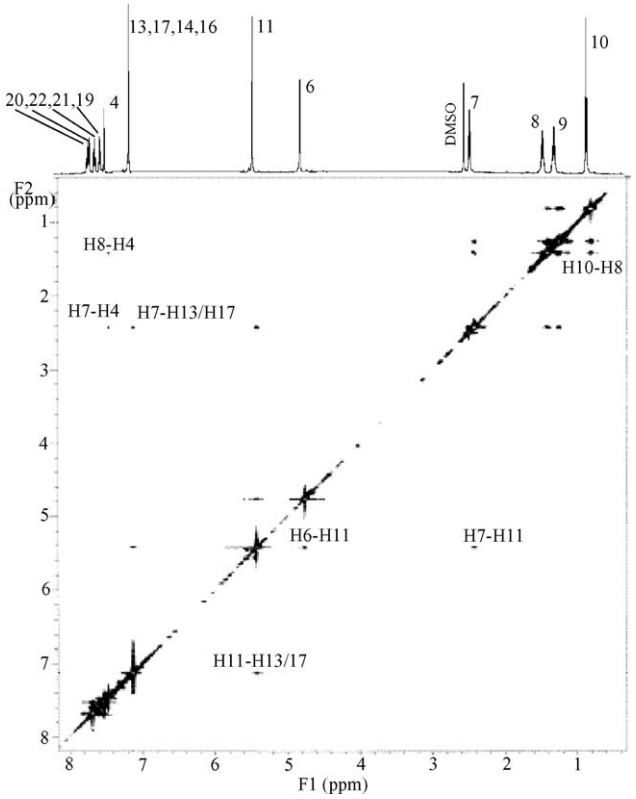


Fig. 3. 2D ROESY spectra of V8.

is AA′BB′ as that of the corresponding losartan but the pattern is not identical. This is attributed either to (i) conformational differences or (ii) environmental effects (different effect of the solvents) [13].

We have applied 2D NOESY technique to losartan and its active metabolite EXP 3174 at various mixing times in order to find the appropriate one for not having spin diffusion effect [15]. We have realized that 2D ROESY experiment of losartan and EXP 3174 have better sensitivity and provide equivalent results using optimum mixing time of 2D NOESY experiments. This is the reason we have adopted ROESY experiment instead of 2D NOESY for fairly structurally similar molecules as it is the molecule of V8.

Table 1
Chemical shifts and J couplings for the protons of V8

| Peak | $\delta$ (ppm) |
|---|---|
| 10 | 0.806 |
| 9 | 1.245 |
| 8 | 1.395 |
| 7 | 2.413 |
| DMSO | 2.495 |
| 6 | 4.754 |
| 11 | 5.410 |
| 13, 14, 16, 17 | 7.116 |
| 4 | 7.453 |
| 19 | 7.515 |
| 21 | 7.584 |
| 22 | 7.659 |
| 20 | 7.682 |

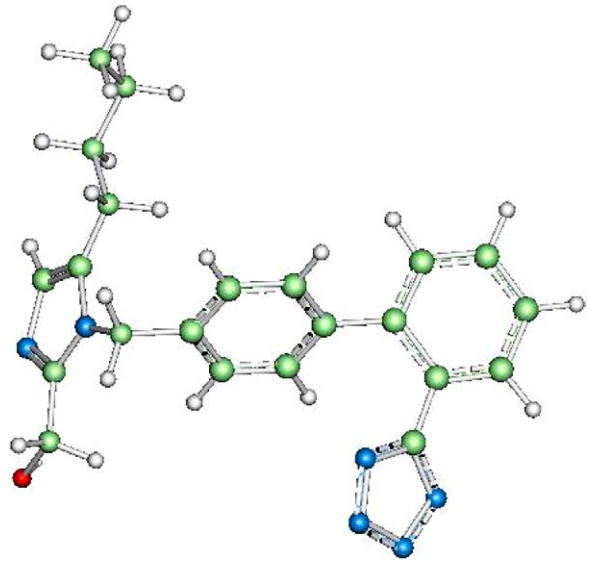

Fig. 4. Low energy conformer of V8 obtained using minimization procedures (Conformer S).

### 3.2. Conformational properties of V8

The important ROEs which reflect the conformational properties of V8 are presented in Table 2. Specifically, H7, H8 and H9 of the butyl chain, all give ROEs with H11, H13/17 and H4. These ROEs reflect the butyl chain spatial preference between the biphenyl system and H4. Such a conformational property differs from the one observed with losartan in which the butyl chain is oriented towards the biphenyl group, favoring Van der Waals interactions.

### 3.3. Conformational analysis

The most important conformational features of V8 are: (i) the conformation of the biphenyl scaffold and the orientation of the tetrazole relative to the imidazole ring; (ii) the orientation of the tetrazole relatively to the attached aromatic ring; (iii) the relative orientation of the imidazole and spacer phenyl ring; (iv) the orientation of the hydroxymethyl group; (v) the conformation and mobility of the butyl chain.

V8 was first minimized using first and second order minimization protocols. Low energy conformers were generated using Random Sampling method and after minimization they were divided into 14 different classes according to the dihedral angles and with an RMSD value equal to 70.6. These conformations were further minimized until reaching a local minimum. Differences between them are summarized in the conformation of the butyl chain, its orientation relatively to the biphenyl system and the orientation of the tetrazole ring in relation to the butyl chain. Conformer S was the lowest energy conformer in accordance to the experimental restraints and is presented in Fig. 4.

#### 3.3.1. Conformation of the biphenyl ring

The critical dihedral angle $\tau_2$ describes the conformational behavior of the biphenyl template by rotation around the

Table 2
ROEs and their intensities for the V8 molecule

| V8 | Protons | Distance (+10%, −10%) | Los.Cor.Dis[a] |
|---|---|---|---|
| 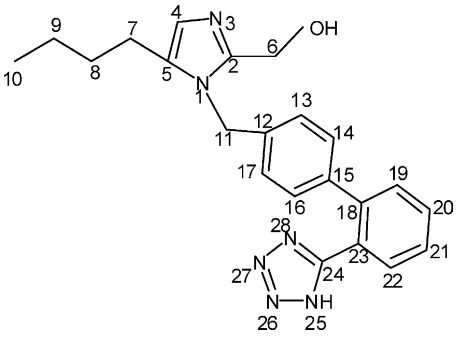 | 10–8 | 2.76 (3.03, 2.48) | 2.78 |
| | 9–7 | 2.53 (2.78, 2.28) | 2.64 |
| | 10–7 | 3.19 (3.51, 2.87) | 3.16 |
| | 11–6 | 2.30 (2.52, 2.07) | 2.70 |
| | 11–7 | 2.31 (2.54, 2.08) | 2.34 |
| | 11–8 | 3.18 (3.50, 2.86) | 3.19 |
| | 11–9 | 3.51 (3.86, 3.16) | 3.86 |
| | 11–13/17 | 2.25 (2.48, 2.03) | 2.38 |
| | 6–13/17 | 2.23 (2.45, 2.01) | 2.94 |
| | 7–13/17 | 2.58 (2.84, 2.32) | 2.54 |
| | 8–13/17 | 3.05 (3.35, 2.74) | 3.38 |
| | 9–13/17 | 3.06 (3.37, 2.76) | 3.09 |
| | 19–14/16 | 1.99 (2.19, 1.79) | 2.07 |
| | 8–4 | 2.39 (2.63, 2.15) | – |
| | 7–4 | 2.67 (2.93, 2.40) | – |
| | 9–4 | 3.17 (3.49, 2.86) | – |

[a] Corresponding distances for the molecule of losartan.

C15–C18 bond and defines the relative orientation of the tetrazole and imidazole rings. Grid scan routine on dihedral $\tau_2$ was applied to conformer S. The potential energy profile as a function of torsion angle $\tau_2$ is shown in Fig. 5. This profile shows that the planes of the two phenyl rings are twisted. Two syn orientations A and D and two anti orientations C and B of tetrazole relative to the imidazole ring are observed. The four conformations together with their $\tau_2$ values are presented in Fig. 5.

### 3.3.2. Orientation of the tetrazole relative to terminal phenyl ring

A grid scan search was performed through rigid rotation around the C23–C24 bond to describe the potential energy as a function of the dihedral angle $\tau_1$. Conformers A–D from previous grid scan search were used as initial structures. The obtained potential energy profiles were found to be similar for all searches. Two energy minima were observed in all conformers located around 100° and −80°. In these conformers tetrazole is inclined relative to the terminal phenyl plane possible to favor π*–π* interactions with the spacer phenyl ring. The energy barrier for the rotation of the tetrazole was found to be approximately 1.5 kcal mol$^{-1}$ suggesting a completely free rotation about the C23–C24 bond.

### 3.4. Relative orientation of the spacer phenyl and imidazole rings

Conformers A–D were the starting structures for another grid scan conformational analysis on $\tau_3$ and $\tau_4$ torsion angles. Dihedral angle $\tau_3$ defines the relative orientation of imidazole to the spacer phenyl ring, while $\tau_4$ describes the transposition of the *n*-butyl and hydroxymethyl groups of the imidazole ring. The

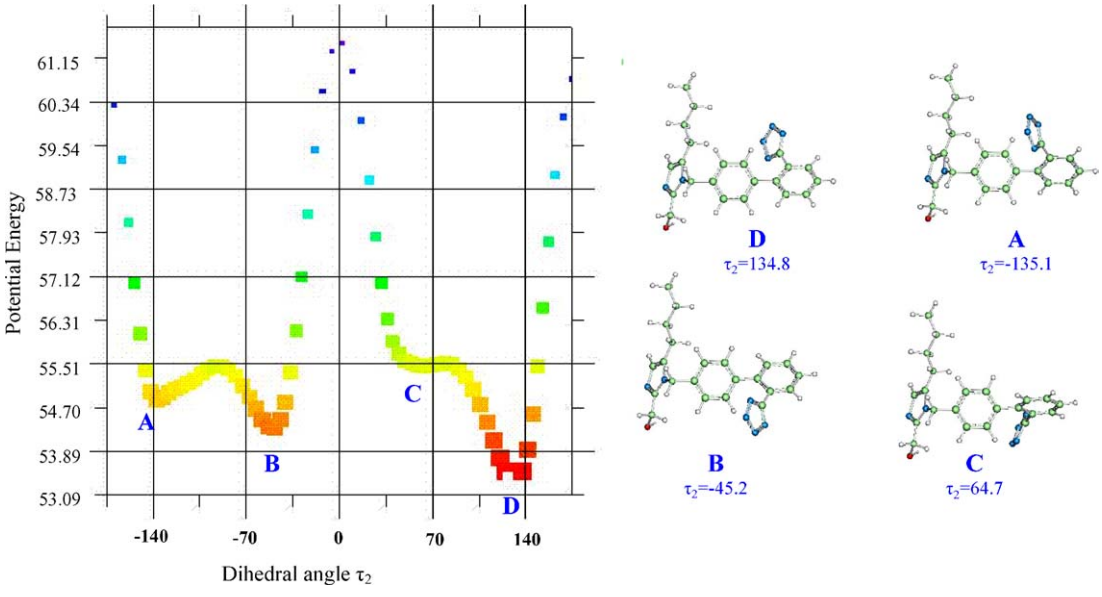


Fig. 5. Conformational energy profile (kcal mol$^{-1}$) as a function of the $\tau_2$ dihedral angle in the biphenyl ring of V8 obtained from a grid scan with increments of 5°.

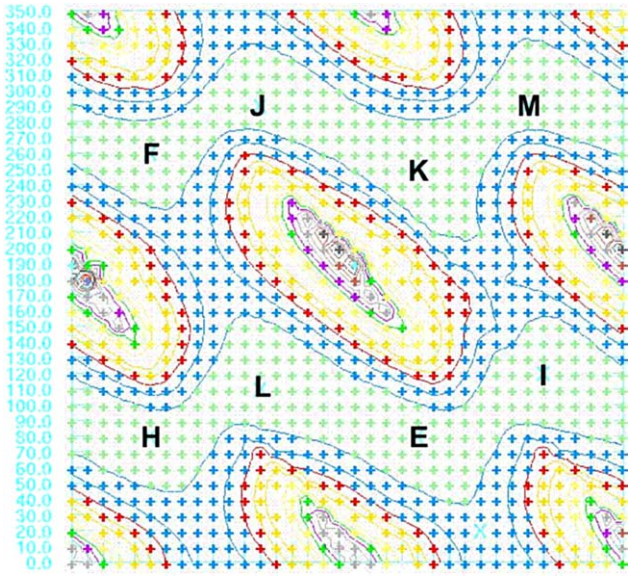


Fig. 6. Contour plot as a function of $\tau_3$ and $\tau_4$ dihedral angles of V8 obtained from a conformational grid scan search analysis with increments of 10°.

four starting conformers A–D gave similar energy contour plots and therefore only representative contour plot for conformer A is presented (Fig. 6). In the contour levels, blue lines represent the low statistical weight conformational levels while the red lines represent the high statistical weight conformational levels. These lines define the relative energy barriers of the molecule to adopt possible bioactive conformations. The corresponding minima of each produced cluster are shown on the plot. The corresponding conformations (E–M) are presented in Fig. 7. They can be divided in three major classes. In the first the butyl chain is oriented away from the biphenyl template (front or back), while in the second and third class it is oriented above and below the biphenyl system. Conformer L (population 10.42%) was in accordance with the majority of experimental ROEs (Table 3).

### 3.4.1. Conformation of the butyl chain

A Monte Carlo conformational analysis was performed through $\tau_7$, $\tau_8$ and $\tau_9$ dihedral angles which define the conformation of the *n*-butyl chain. In the lowest energy structures, the chain was oriented above the phenyl ring. In this category of structures, conformations with either *anti* or *gauche* conformations were obtained. However, the observed ROE between protons 10 and 7 suggests a *gauche* conformation around $\tau_9$ dihedral angle. ROEs between proton 4 and 7, 8, 9 and proton 13 or 17 with 7, 8, 9 indicates that the chain will be located in between protons 4 and 13 or 17.

### 3.4.2. Orientation of the hydroxymethyl group

The conformational mobility of the hydroxymethyl group is restricted by the steric interactions between protons 6 and 13/17 shown by a corresponding ROE between them.

Molecular dynamics experiments using constraints were applied in order to expand the conformational space and increase the probability to generate low energy conformers which agree

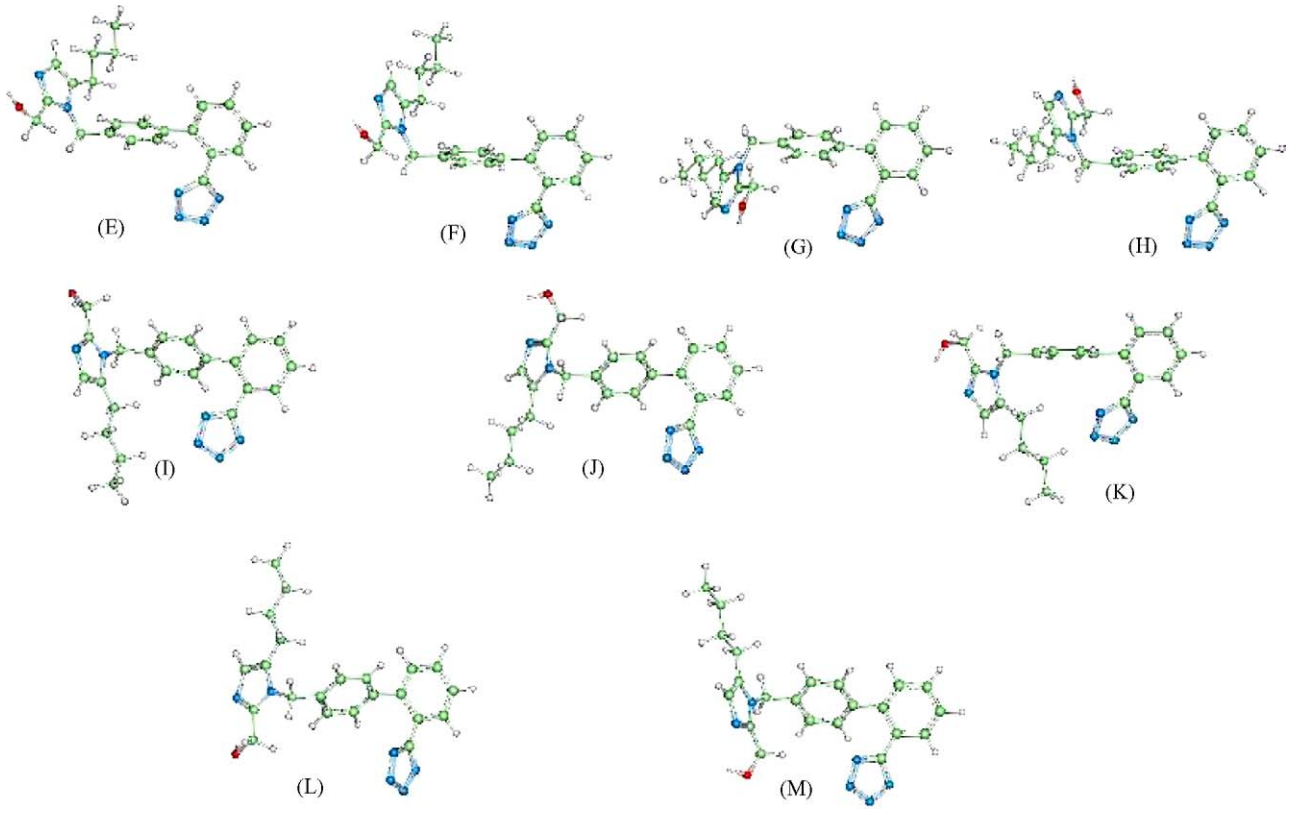


Fig. 7. Low energy conformations derived from a conformational grid scan search analysis between $\tau_3$ and $\tau_4$ dihedral angles.

Table 3
Dihedral angles of the conformers derived using grid scan search between $\tau_3$ and $\tau_4$ dihedrals

| Conformations | Population of 1296 conformations (%) | Relative Energy (kcal mol$^{-1}$) | $\tau_3$ | $\tau_4$ |
|---|---|---|---|---|
| E | 9.26 | 52.87 | 139.22 | −160.62 |
| F | 12.27 | 51.92 | 50.0 | −100.0 |
| G | 14.12 | 51.83 | −140 | 79.97 |
| H | 12.19 | 52.11 | 49.9 | 79.9 |
| I | 14.51 | 51.13 | −60.0 | 119.97 |
| J | 10.42 | 51.65 | 120.0 | −70.0 |
| K | 9.41 | 55.55 | −139.9 | −110 |
| L | 8.26 | 51.47 | 120 | 109.96 |
| M | 9.57 | 51.65 | −69.93 | −70.0 |

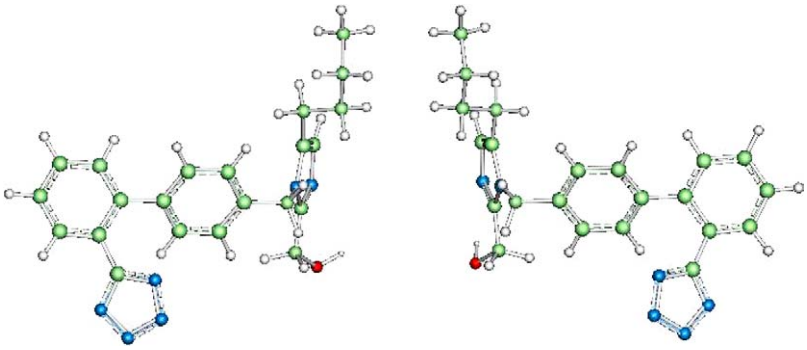

Fig. 8. Proposed bioactive enantiomeric conformers N and N′ of V8 antagonist.

with ROE data. With this procedure we obtained the most important pair of conformational enantiomers best accounting for the ROE data and theoretical calculations. Fig. 8 provides conformer N, and its enantiomer N′. A comparison of their dihedral angles shows that they have $\tau_1$, $\tau_2$ and $\tau_3$ complementary and the rest of diherdrals equal and opposite (Table 4). Such a symmetry in their dihedral angles results in the mirror image relationship.

### 3.5. Superimposition of V8 with losartan

V8 was superimposed with losartan in order to reveal the conformational similarities and differences between the pharmacophoric groups. The atoms N1, C2, C5, C6, C15, C24 included within $\tau_1$–$\tau_5$ dihedral angles, of the two conformational enantiomeric forms (N left and N′ right) of V8 were superimposed with the corresponding conformational enantiomeric forms of losartan described in a previous publication [10].

Table 4
Dihedral angles of the two enantiomeric forms of V8 in DMSO

| Dihedral angles (°) | N conformer | N′ conformer |
|---|---|---|
| $\tau_1$ | −36 | 144 |
| $\tau_2$ | −49 | 131 |
| $\tau_3$ | −80.6 | 100 |
| $\tau_4$ | −87.4 | 87.4 |
| $\tau_5$ | 156.5 | −156 |
| $\tau_6$ | 38.2 | −38.2 |
| $\tau_7$ | −77.7 | 77.7 |
| $\tau_8$ | 179.6 | −179.6 |
| $\tau_9$ | 66.4 | −66.4 |

RMSD value for the superimposition of the N and N′ conformational enantiomers with the corresponding enantiomers of losartan were found to be 0.41 and 0.49 correspondingly implying that $\tau_1$–$\tau_5$ dihedral angles of the two molecules are

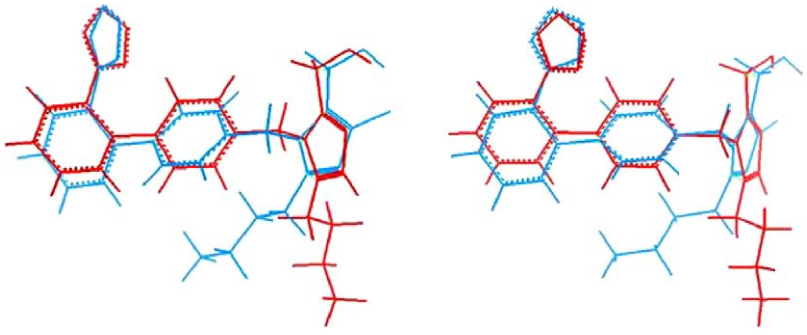

Fig. 9. Superimposition of the two conformational enantiomeric forms (N left and N′ right) of V8 (red) with the corresponding conformational enantiomeric forms of losartan. (For interpretation of the references to colour in this figure legend, the reader is referred to the web version of the article.)

almost identical (Fig. 9). More specifically, the tetrazole rings, the hydroxymethyl groups and the imidazole rings share the same conformational space. The dihedral angle between the two aromatic rings seems to be smaller for the case of V8 while the main conformational difference is observed in the orientation of the butyl chain where for the molecule of V8 seems to favor a position farther of the phenyl rings than the molecule of losartan. This is expected since H7, H8 and H9 of the butyl chain all give ROEs with H11, H13/17 and H4.

## 4. Conclusions

The conformational properties of $AT_1$ antagonists constitute the basis for the stereoelectronic properties which govern their antihypertensive efficacy. In an effort to comprehend these properties we explored the conformations of $AT_1$ antagonists already approved for the treatment of hypertension as well as of novel synthetic compounds. This study revealed conformational similarities and difference between the bioactive molecules V8 and losartan. The major conformational difference between the two molecules is the orientation of the alkyl chain to the biphenyl system. However, the alkyl chains are flexible and explore a substantial conformational space. In this case, such observation prohibits a direct relationship between conformation and bioactivity. The structural differences (relative position of N(3)) and the presence/absence of chlorine in the imidazole moiety) between losartan and V8 may potentially have a significant impact on the binding properties of these molecules to the $AT_1$ receptor. In addition, the conformation of the bound states of these molecules in the biological environment with the receptor may differ and this may also explain their different bioactivity.

The work provided in this article is the first step of a series of studies to be followed by others on the interactions of $AT_1$ antagonists with the membrane bilayers and their docking to the $AT_1$ receptor. Biophysical studies in progress show that the two molecules interact in a different way at membrane level. Docking experiments are also under process. The whole work aims to provide the structural requirements for the design of novel structures with better activity.

## Acknowledgment

The work was funded by the GSRT under the EPAN 4.5 Hercules 2005-2007.

## References

[1] R. Darren, Biochim. Biophys. Acta 207 (1999) 1422.
[2] S. Fermandjian, C. Sakarellos, F. Piriou, M. Juy, F. Toma, H.L. Thanh, K. Lintner, M.C. Khoslia, R.R. Smeby, F.M. Bumpus, Biopolymers 22 (1983) 227.
[3] P.B.M.W.M. Timmermans, P.C. Wong, A.T. Chiu, W.F. Herblin, Trends Pharmacol. Sci. 12 (1991) 55.
[4] R. Wexler, W. Greenlee, J. Irvin, M. Coldberg, K. Prendergast, R. Smith, P. Timmermans, J. Med. Chem. 39 (1996) 625.
[5] J.V. Duncia, A.T. Chiu, D.J. Carini, G.B. Gregory, A.L. Johnson, W.A. Price, F.J. Wells, P.C. Wong, J.C. Calabrese, P.B.M.W.M. Timmermans, J. Med. Chem. 33 (1990) 1312.
[6] J.V. Duncia, D.J. Carini, A.T. Chiu, A.L. Johnson, W.A. Price, P.C. Wong, R.R. Wexler, P.B.M.W.M. Timmermans, Med. Res. Rev. 12 (1992) 149.
[7] P. Zoumpoulakis, S.G. Grdadolnik, J. Matsoukas, T. Mavromoustakos, J. Pharm. Biomed. Anal. 28 (2002) 125–135.
[8] L. Polevaya, T. Mavromoustakos, P. Zoumpoulakis, S.G. Grdadolnik, P. Roumelioti, N. Giatas, I. Mutule, T. Kevish, D. Vlahakos, E. Iliodromitis, D. Kremastinos, J. Matsoukas, Bioorg. Med. Chem. 9 (2001) 1639–1647.
[9] P. Zoumpoulakis, A. Zoga, P. Roumelioti, N. Giatas, S.G. Grdadolnik, E. Iliodromitis, D. Vlahakos, D. Kremastinos, J.M. Matsoukas, T. Mavromoustakos, J. Pharm. Biomed. Anal. 31 (2003) 833–844.
[10] T. Mavromoutakos, A. Kolocouris, M. Zervou, P. Roumelioti, J. Matsoukas, R. Weisemann, J. Med. Chem. 42 (1999) 1714–1722.
[11] P. Zoumpoulakis, I. Daliani, M. Zervou, I. Kyrikou, E. Siapi, G. Lamprinidis, E. Mikros, T. Mavromoustakos, Chem. Phys. Lipids 125 (2003) 13–25.
[12] T. Mavromoustakos, A. Kapou, N.P. Benetis, M. Zervou, Drug Des. Rev. Online 1 (3) (2004) 235–245.
[13] T. Mavromoustakos, M. Zervou, P. Zoumpoulakis, I. Kyrikou, N.P. Benetis, L. Polevaya, P. Roumelioti, N. Giatas, A. Zoga, P. Moutevelis Minakakis, A. Kolocouris, D. Vlahakos, S. Golic Grdadolnik, J. Matsoukas, Curr. Top. Med. Chem. 4 (2004) 385–401.
[14] K.P. Marathias, B. Agroyannis, T. Mavromoustakos, J. Matsoukas, D.V. Vlahakos, Curr. Top. Med. Chem. 4 (2004) 483–486.
[15] M. Zervou, Ph.D. Thesis, University of Patras-Greece, 2001.
[16] A. Zoga, Ph.D. Thesis, University of Patras-Greece, 2004.
[17] M. Rance, O.W. Sorensen, G. Bodenhausen, G. Wagner, R.R. Ernst, K. Wutrich, Biochem. Biophys. Res. Commun. 117 (1983) 479–485.
[18] G. Bodenhausen, D.J. Ruben, Chem. Phys. Lett. 69 (1980) 185–189.
[19] W. Wilker, D. Leibfritz, R. Kerrsebaum, W. Bermel, Magn. Reson. Chem. 31 (1983) 479–485.
[20] J. Jeener, B.H. Meier, P. Bachmann, R.R. Ernst, J. Chem. Phys. 71 (1979) 4546–4553.
[21] A. Bax, M.F. Summers, J. Am. Chem. Soc. 108 (1986) 2093–2094.
[22] W. Bermel, K. Wagner, C. Griesinger, J. Magn. Reson. 83 (1989) 223–232.